Fluctuation-Induced Phase Separation in Metric and Topological Models of Collective Motion

David Martin, Hugues Chaté, Cesare Nardini, Alexandre Solon, Julien Tailleur, and Frédéric Van Wijland

Fluctuation-induced phase separation in metric and topological models of collective motion

David Martin,[1] Hugues Chaté,[2,3] Cesare Nardini,[2] Alexandre Solon,[4] Julien Tailleur,[1] and Frédéric Van Wijland[1]

[1]*Universit de Paris, Laboratoire Matière et Systèmes Complexes (MSC), UMR 7057 CNRS, F-75205 Paris, France*
[2]*Service de Physique de l'Etat Condensé, CEA, CNRS Université Paris-Saclay, CEA-Saclay, 91191 Gif-sur-Yvette, France*
[3]*Computational Science Research Center, Beijing 100193, China*
[4]*Sorbonne Université, CNRS, Laboratoire Physique Théorique de la Matière Condensée, 75005 Paris, France*
(Dated: December 23, 2020)

We study the role of noise on the nature of the transition to collective motion in dry active matter. Starting from field theories that predict a continuous transition at the deterministic level, we show that fluctuations induce a density-dependent shift of the onset of order, which in turns changes the nature of the transition into a phase-separation scenario. Our results apply to a range of systems, including models in which particles interact with their 'topological' neighbors that were believed so far to exhibit a continuous onset of order. Our analytical predictions are confirmed by numerical simulations of fluctuating hydrodynamics and microscopic models.

Within active matter studies, the transition to collective motion is a problem of both historical and paradigmatic value, which has led to a wealth of theoretical [1–5], numerical [6–8] and experimental works [9–12]. Thanks to their simplicity, dry polar flocks, in which self-propelled particles stochastically and locally align their velocities, fuel an extensive research field [5–7, 13–22]. Beyond the sole realm of active matter, the statistical-physics modelling of collective motion has disseminated to topics as diverse as animal behavior [23–25], human crowd dynamics [26], biology [11, 27–30], or swarm robotics [31].

The transition to collective motion is best understood in the context of *metric* models, in which particles align with neighbors within a finite distance. At the microscopic level, the nature of the transition is now well established [5, 7, 8]. It takes the form of a phase separation between a disordered gas/paramagnetic phase and a polarly ordered liquid/ferromagnetic phase, separated by a coexistence region where traveling bands are observed [32]. On the contrary, the transition is believed to be continuous for 'metric-free' systems [33, 36, 38, 41], where interactions between agents is not decided based on their relative distance [24, 34, 35, 37, 39, 40]. For these models, often referred to as *topological* [37], traveling bands have indeed not been reported so far. Topological models play an important role thanks to their relevance to studies of groups of animals [24, 34, 35, 39] or pedestrians [42], where visual cues dominate metric ones. They are also the natural choice to model confluent tissues where topological neighborhoods determine interactions [29, 40, 43–45]. Existing numerical results on the transition are scarce and limited to particles aligning with their Voronoi neighbors [33] or their k-nearest neighbors [38, 46].

These microscopic-level results have been rationalized using deterministic hydrodynamic theories, which typically couple a density field ρ and an order parameter field [3, 5, 47–50]. In the metric case, the phase-separation scenario can be understood by considering their dynamics in one spatial dimension, a minimal model of which is given by

$$\partial_t \rho = D\partial_{xx}\rho - v\partial_x m \tag{1}$$
$$\partial_t m = D\partial_{xx}m - v\partial_x \rho - \mathcal{F}(\rho, m) . \tag{2}$$

Here, m is akin to a magnetisation field in a spin system and $\mathcal{F}(\rho, m) = \alpha m + \gamma\frac{m^3}{\rho^2}$ is a Landau term that controls ferromagnetic alignment [5]. Historically, Eqs (1) and (2) were derived as a mean-field description of the active Ising model (AIM) [5]. Here, D stems from the random hopping of particles and is the same for m and ρ, v stems from their self propulsions, while α and γ control the alignment. Many similar hydrodynamic models have been proposed or derived in one and two dimensions [2–5, 12, 47, 50]. All lead to the same conclusion: the first-order, phase-separation nature of the transition stems from the density-dependence of the linear term: $\alpha = \alpha(\rho)$. A density-dependent threshold—or critical temperature, to continue the ferromagnetic analogy—such that $\alpha'(\rho) \neq 0$ leads to the phase-separation scenario. The latter is characterized by two main features: homogeneous ordered profiles are linearly unstable close to the transition, when $\alpha \lesssim 0$, and this instability leads to the emergence of traveling bands [7, 48, 52]. In the topological case, mean-field descriptions of Voronoi-based [36] and k-nearest-neighbor models [38] both lead to a density-independent critical temperature, hence predicting a continuous onset of order. This result is compatible with the observation that doubling the distance between all particles, and hence reducing the particle density, does not impact the aligning dynamics. Topological models are thus expected to be much less sensitive to density variations and the current understanding is that they constitute a universality class distinct from metric models.

In this Letter, we show that the continuous scenario does not survive incorporating fluctuations. To do so, we construct a hydrodynamic description of metric-free models in which particles align with their k nearest neighbors [24]. This requires preserving the topological nature of the interactions at the coarse-grained level, which we achieve by means of a non-local orientation field. We show that, at the deterministic level, the transition is predicted to be continuous. Dressing the model with noise, however, leads to a renormalized density-dependent critical temperature that signals a phase-separation scenario. This analytical result is supported by microscopic simulations. Finally, we show that measuring the density-dependency of the onset of order is a simple quantitative test which allows predicting the nature of the transition,

hence solving a long-standing numerical difficulty [7, 33, 46]. All calculations below are based on the one-dimensional hydrodynamic theory (1)-(2) and its topological generalization. Our results can be extended to two dimensions and to other hydrodynamic models, as well as to more general topological constraints [51]. The generalization of the results presented in this Letter will be fully detailed in a later publication [55]. We complement our analytical approach by numerical simulations, mostly in 2D, which are all detailed in [51]

Fluctuation-induced first-order transitions. For clarity, we first show that dressing the 'metric' PDEs (1)-(2) with noise generically yields a renormalized density-dependent critical temperature, hence leading to phase separation, before considering the topological case. This allows presenting our analytical approach in a simpler framework. We consider α independent of ρ to show that the corresponding hydrodynamic descriptions, derived in some scaling limits [53, 54], are unstable to fluctuations. We complement Eq. (2) with a noise term

$$\partial_t m = D\partial_{xx}m - v\partial_x\rho - \mathcal{F}(\rho, m) + \sqrt{2\sigma\rho}\,\eta\,,\quad (3)$$

where $\eta(x,t)$ is a zero-mean delta-correlated Gaussian white noise field. Note that, hereafter, $\rho(x,t)$ and $m(x,t)$ represent fluctuating fields. The order parameter $m(x,t)$ represents the sum of the orientations of particles located around position x. The noise acting on $m(x,t)$ will thus be multiplicative; it describes the fluctuations of a sum over $\propto \rho$ particles and we take it proportional to $\sqrt{\rho(x,t)}$. We now construct the hydrodynamics of the average fields $\rho_0(x,t) = \langle\rho(x,t)\rangle$ and $m_0(x,t) = \langle m(x,t)\rangle$ to leading order in the noise strength σ, where brackets represent average over noise realizations. In principle, we could also complement Eq. (1) with a conserved noise. The latter is expected to be subdominant at large scales and we ignore it here, although our approach can be extended to this case. Introducing $\delta\rho = \rho - \rho_0$ and $\delta m = m - m_0$, the dynamics of ρ_0 and m_0 can be approximated as

$$\partial_t\rho_0 = D\partial_{xx}\rho_0 - v\partial_x m_0 \quad (4)$$

$$\partial_t m_0 = D\partial_{xx}m_0 - v\partial_x\rho_0 - \mathcal{F}(\rho_0, m_0)$$
$$-\frac{\partial^2\mathcal{F}}{\partial m^2}\frac{\langle\delta m^2\rangle}{2} - \frac{\partial^2\mathcal{F}}{\partial\rho^2}\frac{\langle\delta\rho^2\rangle}{2} - \frac{\partial^2\mathcal{F}}{\partial m\partial\rho}\langle\delta m\delta\rho\rangle \quad (5)$$

To close Eqs. (4) and (5), we need to compute $\langle\delta m^2\rangle$, $\langle\delta\rho^2\rangle$, $\langle\delta m\delta\rho\rangle$ as functions of ρ_0 and m_0. In the small noise limit, the fluctuations $\delta\rho$ and δm are assumed to be small so that we compute these correlators at the linear, Gaussian fluctuations level [56–59]. The dynamics of $\delta\rho(x,t)$, $\delta m(x,t)$ then read

$$\partial_t\delta\rho = D\partial_x^2\delta\rho - v\partial_x\delta m \quad (6)$$

$$\partial_t\delta m = D\partial_x^2\delta m - v\partial_x\delta\rho - \frac{\partial\mathcal{F}}{\partial\rho}\delta\rho - \frac{\partial\mathcal{F}}{\partial m}\delta m + \sqrt{2\sigma\rho_0}\,\eta \quad (7)$$

For $\alpha \neq 0$, this linear system of equations leads to bounded fluctuations of $\delta\rho$, δm around the homogeneous solutions of Eq. (1) and (2). It can be solved in Fourier space and the correlators appearing in (5) can be obtained explicitly as integrals
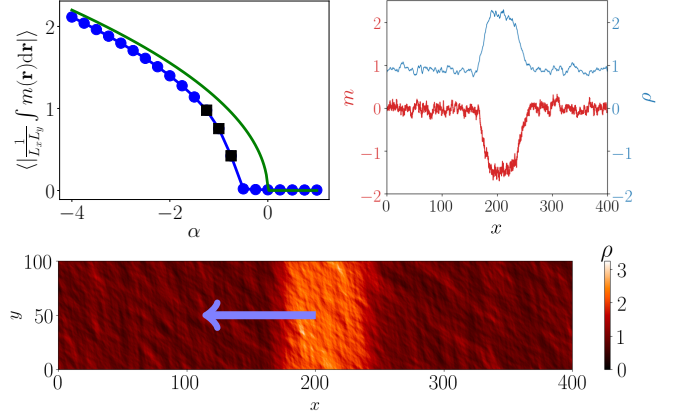

FIG. 1. Simulations of the 2D generalization of Eqs. (1) and (3) detailed in [51]. **Top left**: Average magnetisation as α is varied. The transition occurs at $\alpha_c < 0$, shifted from the mean-field prediction (green line). At the onset of order, inhomogeneous profiles (black squares) separate homogeneous ordered and disordered phases (blue dots). Parameters: $D = v = \gamma = \sigma = 1$, $dx = 0.5$, $dt = 0.01$, $L_x = 400$, $L_y = 40$, $\bar\rho \equiv N/(L_xL_y) = 1.1$. **Bottom**: A snapshot close to the transition shows an ordered traveling band in a disordered background. **Top right**: The corresponding density and magnetization fields averaged along y. Parameters: same as before up to $L_y = 100$, $dx = 0.1$, $\alpha = -0.9$.

over k space, e.g. $\langle\delta m^2\rangle = \int dk\langle\delta m_k\delta m_{-k}\rangle/(2\pi)$ [51]. The alignment terms in Eq. (5) can then, consistently with the approximation leading to a Landau form, be expanded as $\tilde{\mathcal{F}}(\rho_0, m_0) = \tilde\alpha m_0 + \tilde\gamma m_0^3/\rho_0^2$. Fluctuations have thus, to this order in σ, dressed α and γ into $\tilde\alpha$ and $\tilde\gamma$. For a given set of parameters, the integrals over k space can be computed numerically. It is, however, more enlightening to compute them explicitly in the high-temperature phase, where $\alpha > 0$. The precise expression of $\tilde\gamma$ is irrelevant for our purpose, and is presented in [51]. The linear term is renormalized into

$$\tilde\alpha = \alpha + \frac{3\sigma\gamma}{4\rho_0 v}f\left(\frac{\alpha D}{v^2}\right) \text{ with } f(u) = \frac{\sqrt{2/u} + \sqrt{1+u}}{2+u} \quad (8)$$

Importantly, $\tilde\alpha$ now depends explicitly on the density [60]. To first order in σ, fluctuations thus renormalize the continuous transition predicted by Eqs. (1) and (2) into the standard liquid-gas phase separation. Note that higher orders in σ have no reason to cancel the dependence of $\tilde\alpha$ on density and we thus expect our conclusions to hold non-perturbatively in σ.

To confirm our predictions, we carried out simulations of the scalar 2D generalization of the stochastic PDEs (1) and (3) [51]. The continuous transition predicted by Eqs. (1) and (2) is replaced by the standard liquid-gas framework [5, 61], as shown in Fig. 1 by the emergence of traveling-band solutions.

Field theory for topological interactions. The study of the dynamics (1) and (3) thus showed that fluctuations generically make the transition to collective motion first order in metric models. This applies, in particular, to the hydrodynamic theory proposed for Voronoi-based interactions in [36]. We now

propose an alternative hydrodynamic description which preserves the topological nature of the interactions at the coarse-grained level. To do so, we focus on models in which particles align with their k nearest neighbors, which are commonly used to model animal and human behavior [24, 34, 35, 39, 42]. Numerically, the transition has been reported to be continuous in systems of linear sizes of order $L \sim 10^2$, for up to $N = 10^4 - 10^5$ particles [38, 46]. To proceed, we introduce a coarse-grained field $y(x)$ which measures the interaction range of a particle at x:

$$\int_{x-y(x)}^{x+y(x)} \rho(z)\mathrm{d}z = k \ . \quad (9)$$

Particles at position x then align with a 'topological' field $\bar{m}(x,t)$ computed over their k nearest neighbours through

$$\bar{m}(x) = \frac{1}{k} \int_{x-y(x)}^{x+y(x)} m(z)\mathrm{d}z \ . \quad (10)$$

Doubling the distance between particles does not alter the values of $\bar{m}(x)$, consistent with microscopic topological models [24, 33]. To construct the topological counterpart of the Landau term $\mathcal{F}(\rho,m)$ appearing in the metric dynamics, let us recall how the latter is constructed from microscopic models. In a ferromagnetic context, $\mathcal{F}$ can be seen as the small-magnetisation expansion of a more complex function $\mathcal{F}_{\text{ferro}} = 2m\cosh(\beta p) - 2\rho\sinh(\beta p)$, where $p = m/\rho$ is the local magnetisation per particle and β the inverse temperature. The fields ρ and m enter $\mathcal{F}_{\text{ferro}}$ through counting statistics, $(\rho \pm m)/2$ representing the local densities of particles with plus or minus spins. The field p, on the other hand, enters via the aligning rate at which a spins s flips, e.g. $W(s \to -s) = \Gamma\exp(-\beta sp)$. When particles align stochastically with a topological field $\bar{m}$, the Landau term thus simply becomes $\mathcal{F}_{\text{ferro}} = 2m\cosh(\beta\bar{m}) - 2\rho\sinh(\beta\bar{m})$. Expanding to third order in the fields then yields:

$$\mathcal{F}_{\text{topo}}(m, \rho, \beta) = \Gamma\left(2m - 2\rho\beta\bar{m} - \frac{\rho\beta^3}{3}\bar{m}^3 + \beta^2 m\bar{m}^2\right) \quad (11)$$

in which, for simplicity, we retain β as the sole control parameter. At mean-field level, our topological field theory is thus given by Eq. (1) and (2), with $\mathcal{F}$ replaced by $\mathcal{F}_{\text{topo}}$.

Homogeneous solutions ρ_0, m_0 correspond to $y(x) = k/(2\rho_0)$ and $\bar{m} = m_0/\rho_0$. The linear term in $\mathcal{F}_{\text{topo}}$ then reduces to $2\Gamma(1-\beta)m_0$, leading to a density-independent transition at $\beta_m = 1$. Linear stability analysis of the homogeneous solutions then shows that disordered and ordered solutions are linearly stable for $\beta < \beta_m$ and $\beta > \beta_m$, respectively [51]. Our topological field theory thus predicts a continuous transition at the mean-field level.

Let us now assess the effect of dressing the dynamics of the order parameter with noise: we consider the stochastic dynamics (1) and (3), albeit with $\mathcal{F}$ replaced by $\mathcal{F}_{\text{topo}}$. Here also, the noise is multiplicative and proportional to $\sqrt{\rho(x,t)}$ since $m(x,t)$ is the sum of the orientations of particles located around position x. To construct the dynamics of the
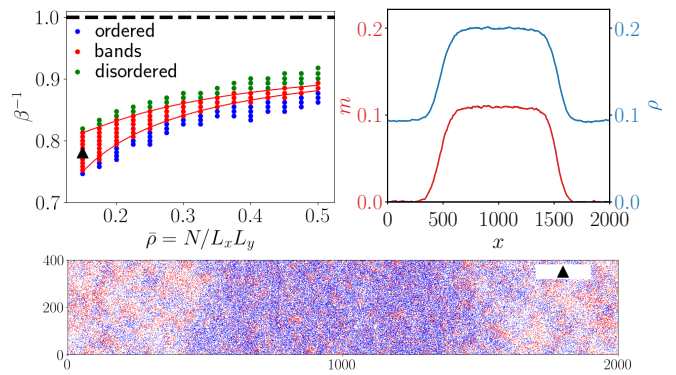

FIG. 2. **Top Left:** Phase diagram of the microscopic topological model defined in Eqs. (13) and (14). The homogeneous ordered (blue) and disordered (green) regions are separated by a coexistence phase (red). The mean-field critical temperature is $\beta = 1$ (dashed-lined). The red lines are guide to the eyes which show how the transitions shift as the mean density varies. **Bottom:** Snapshot of a propagating band corresponding to the black triangle in the phase diagram. Blue and red particles correspond to positive and negative spin. The corresponding density and magnetization fields, averaged over y and time, are shown in the top-right panel. Parameters: $D = 8$, $L_y = 400$, $L_x = 2000$, $k = 3$, $\Gamma = 0.5$, $v = 0.9$.

average fields ρ_0 and m_0 perturbatively in σ, we first stress that Eq. (9) directly enslaves the field $y(x)$ to $\rho(x)$. There are thus, again, only two independent fields, $\rho(x,t)$ and $m(x,t)$, so that Eq. (7) is still valid, up to $\mathcal{F} \to \mathcal{F}_{\text{topo}}$. The expression of $\mathcal{F}_{\text{topo}}$ being, however, more complicated than in the metric case, the algebra is correspondingly more involved. We detail in [51] the renormalization of the linear part of $\mathcal{F}_{\text{topo}}$, which controls the nature of the transition. To first order in the noise strength σ, we find

$$(\beta - 1)m_0 \to \left[\beta - 1 - \frac{\sigma}{k}g\left(\beta, \frac{\Gamma k}{v\rho_0}, \frac{\Gamma D}{v^2}\right)\right]m_0 \ , \quad (12)$$

with g a positive function whose expression is provided as an integral in [51].

Importantly, the linear term in the aligning dynamics of m_0 has again become density-dependent, hence predicting a phase-separation scenario. This is confirmed by numerical simulations of (1) and (3) with $\mathcal{F} \to \mathcal{F}_{\text{topo}}$, which again reveal the existence of inhomogeneous propagating bands [51]. Our results thus also predict a fluctuation-induced phase-separation scenario for topological models.

Microscopic models with k-nearest-neighbors interactions. To test the above predictions, we first consider an off-lattice active Ising model [5, 61] in which N particles move in an $L_x \times L_y$ domain with periodic boundary conditions. Each particle carries a spin $s_i = \pm 1$ and evolves according to the Langevin dynamics

$$\dot{\mathbf{r}}_i = s_i\, v_0\, \hat{\mathbf{x}} + \sqrt{2D}\boldsymbol{\eta}_i \ , \quad (13)$$

where v_0 sets the self-propulsion speed and D sets the strength of the unit-variance Gaussian white noise $\boldsymbol{\eta}_i$. Spins flip from
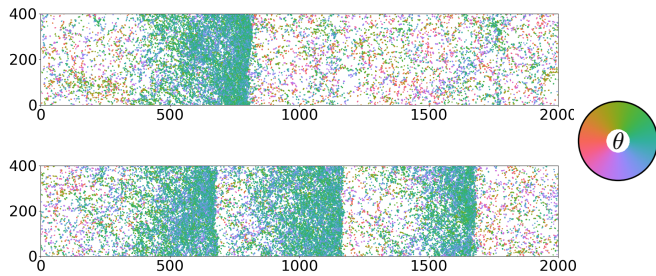
FIG. 3. Simulations of the topological Vicsek model in 2D. At small noise, the system is disordered at low enough densities. Increasing the density then leads to an onset of order accompanied by propagating bands. Particles align with their $k = 3$ nearest neighbors. Parameters : $L_x = 2000$, $L_y = 400$, $\sigma = 0.08$, $k = 3$, $v_0 = 0.2$, $\Delta t = 1$, $\bar{\rho} = 0.25$ (top) and $\bar{\rho} = 0.4$ (bottom).
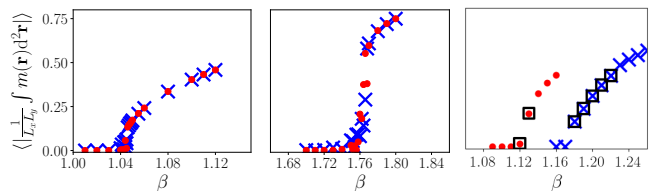

FIG. 4. Magnetization vs inverse temperature β for the RAM (left), the LAM (center), and the topological model (13)-(14) (right). Only the latter exhibits traveling bands (black squares). Blue crosses and red dots correspond to mean densities $\bar{\rho} = 0.25$ and $\bar{\rho} = 0.5$, respectively. Parameters: $L_x = 2000$, $L_y = 400$, $D = 8$, $v = 0.9$, $\Gamma = 0.5$, $k = 3$. For LAM, $k = 4$.

s_i to $-s_i$ at rate $W(s_i)$ given by

$$W(s_i) = \Gamma e^{-\beta s_i \bar{m}_i}, \quad \text{where} \quad \bar{m}_i = \frac{1}{k} \sum_{j \in \mathcal{N}_i} s_j , \qquad (14)$$

where $\mathcal{N}_i$ is the set of the k-nearest neighbours of particle i and $\bar{m}_i$ their average magnetization. Note that a mean-field treatment of the aligning dynamics (14) indeed leads to Eq. (11). In agreement with our predictions, the model exhibits a first order transition to collective motion, akin to a liquid-gas phase separation: the onset of order at $\beta \gtrsim \beta_c(\rho_0)$ occurs through the emergence of an ordered propagating band (Fig. 2). Unlike the mean-field critical temperature, the boundaries of the coexistence region show a clear dependence on the mean density $\bar{\rho}$.

To probe the generality of our results, we then implemented a topological version of the Vicsek model [6, 7] in which the particles align with their k nearest neighbors. We considered N point particles carrying unit propulsion vectors $\mathbf{u}_i$ and moving in a $L_x \times L_y$ domain with periodic boundary conditions. At every time step, the particles align with the average direction of their k nearest neighbors:

$$\arg\left[\mathbf{u}_i\right] \to \arg\left[\frac{1}{k} \sum_{j \in \mathcal{N}_i} \mathbf{u}_j\right] + \sigma\eta , \qquad (15)$$

where η is uniformly drawn in $[-\pi, \pi]$. The particles then move a distance $v_0\Delta t$ along their propulsion vector. Propagating bands are observed close to the onset of collective motion (Fig. 3). Overall, despite being usually considered resilient to density fluctuations, the topological interactions studied in this article thus lead to a phase-separation scenario.

A numerical test of the nature of the transition. Since the introduction of the Vicsek model, determining numerically the nature of the transition has proven a difficult task [7]. The weakly first-order nature of the transition indeed challenges standard methods: in finite systems, the variations of the order parameter as a function of control ones (noise, density, etc.) often misleadingly suggests a second order scenario.

Our results suggest an efficient alternative: measuring the dependency of the onset of order on the average density. We illustrate this by contrasting our topological model with simpler ones in which the aligning dynamics is disconnected from spatial positions, hence trivially ensuring that the transition remains continuous.

We consider N scalar spins moving in a $L_x \times L_y$ domain with periodic boundary conditions according to the Langevin equation (13) with two different aligning dynamics [62]. In the Random Alignment Model (RAM), the aligning dynamics is given by (14), with $\bar{m}_i$ computed over k spins chosen at random at every time step. In the Loyal Alignment Model (LAM), on the contrary, alignment occurs with the same set of k neighbours throughout the simulations, irrespective of the particle positions. In our simulations, we chose $k = 4$ and assigned to each particle its nearest neighbours on an initial square lattice. Simulations of both systems lead to continuous transitions, without the emergence of inhomogeneous phases. Figure 4 shows that the behaviors of the global magnetization as the temperature is varied are hard to distinguish between LAM, RAM and our topological microscopic model. Repeating these measurements at different densities however reveals a density-dependence of the onset of order in the latter case, but not in LAM & RAM. Measuring β_c as $\bar{\rho}$ varies thus constitutes a simple and robust test of the nature of the transition.

Conclusion. In this Letter, we have set up a field-theoretical approach which captures the impact of noise on the hydrodynamic description of the transition to collective motion. Introducing a continuous description of metric-free models, we have shown that, contrary to common belief, the transition in topological models is not critical and involves a phase-separation scenario, hence falling into the same universality class as metric models. This fluctuation-induced phase separation relies on a noise-induced dependency of the onset of order on the average density, which can be exploited in numerical simulations to assess the nature of the transition. This is a more stringent test than measuring putative critical exponents, which are unlikely to distinguish weakly-first-order transitions from the liquid-gas scenario. Note that our topological field theory addressed the case of k-nearest neighbours interaction and one may wonder whether our conclusion holds

for more generic topological fields, e.g. describing Voronoi neighbours. As shown in [51], dimensional analysis suggests that our results should hold for a broader class of topological fields $\bar{m}(x) = \mathcal{G}(x, [\rho, m])$, whose numerical studies are deferred to a longer account of our work [55].

Furthermore, while we have here focused on theoretical and numerical approaches, the coefficients of the linearized Toner-Tu equations have been measured experimentally in flocks of Quincke rollers [63]. Determining the functional form of $\alpha(\rho)$ could thus also be a direct experimental probe of the order of the transition in systems in which finite-size effects would prevent the existence of polar bands.

We have here studied the framework of polar flocks, but our methods can be exported to a broader class of problems, from nematic alignment to models in which the coupling between density and alignment is qualitatively altered, from Malthusian [22] to incompressible [64] or Lévy flocks [65]. Finally, describing non-local interactions at the field-theoretical level had proven a difficult problem so far, which our topological theory has overcome. The relevance of such non-local interactions goes beyond active matter: from cellular [29, 40, 43–45] to social interactions [42, 66]; we hope that our methodology will help build coarse-grained descriptions of metric-free problems in other fields.

---

[1] J. Toner and Y. Tu, Physical Review Letters **75**, 4326 (1995).

[2] J. Toner, Y. Tu, and S. Ramaswamy, Annals of Physics **318**, 170 (2005).

[3] E. Bertin, M. Droz, and G. Grégoire, Physical Review E **74**, 022101 (2006).

[4] S. Mishra, A. Baskaran, and M. C. Marchetti, Physical Review E **81**, 061916 (2010).

[5] A. Solon and J. Tailleur, Physical Review Letters **111**, 078101 (2013).

[6] T. Vicsek, A. Czirók, E. Ben-Jacob, I. Cohen, and O. Shochet, Physical Review Letters **75**, 1226 (1995).

[7] G. Grégoire and H. Chaté, Physical Review Letters **92**, 025702 (2004).

[8] H. Chaté, F. Ginelli, G. Grégoire, and F. Raynaud, Phys. Rev. E **77**, 046113 (2008).

[9] V. Narayan, S. Ramaswamy, and N. Menon, Science **317**, 105 (2007).

[10] J. Deseigne, O. Dauchot, and H. Chaté, Physical Review Letters **105**, 098001 (2010).

[11] V. Schaller, C. Weber, C. Semmrich, E. Frey, and A. R. Bausch, Nature **467**, 73 (2010).

[12] A. Bricard, J.-B. Caussin, N. Desreumaux, O. Dauchot, and D. Bartolo, Nature **503**, 95 (2013).

[13] F. Ginelli, F. Peruani, M. Bär, and H. Chaté, Physical Review Letters **104**, 184502 (2010).

[14] F. Peruani, T. Klauss, A. Deutsch, and A. Voss-Boehme, Physical Review Letters **106**, 128101 (2011).

[15] V. Dossetti and F. J. Sevilla, Physical Review Letters **115**, 058301 (2015).

[16] A. Morin, N. Desreumaux, J.-B. Caussin, and D. Bartolo, Nature Physics **13**, 63 (2017).

[17] L. Chen, C. F. Lee, and J. Toner, New Journal of Physics **20**, 113035 (2018).

[18] F. A. Lavergne, H. Wendehenne, T. Bäuerle, and C. Bechinger, Science **364**, 70 (2019).

[19] B. Mahault, F. Ginelli, and H. Chaté, Physical Review Letters **123**, 218001 (2019).

[20] D. Geyer, D. Martin, J. Tailleur, and D. Bartolo, Physical Review X **9**, 031043 (2019).

[21] H. J. Charlesworth and M. S. Turner, Proceedings of the National Academy of Sciences **116**, 15362 (2019).

[22] L. Chen, C. F. Lee, and J. Toner, arXiv preprint arXiv:2001.01300 (2020).

[23] J. Buhl, D. J. Sumpter, I. D. Couzin, J. J. Hale, E. Despland, E. R. Miller, and S. J. Simpson, Science **312**, 1402 (2006).

[24] M. Ballerini, N. Cabibbo, R. Candelier, A. Cavagna, E. Cisbani, I. Giardina, V. Lecomte, A. Orlandi, G. Parisi, A. Procaccini, M. Viale, and V. Zdravkovic, Proceedings of the National Academy of Sciences **105**, 1232 (2008), https://www.pnas.org/content/105/4/1232.full.pdf.

[25] A. Cavagna, D. Conti, C. Creato, L. Del Castello, I. Giardina, T. S. Grigera, S. Melillo, L. Parisi, and M. Viale, Nature Physics **13**, 914 (2017).

[26] N. Bain and D. Bartolo, Science **363**, 46 (2019).

[27] H.-P. Zhang, A. Beer, E.-L. Florin, and H. L. Swinney, Proceedings of the National Academy of Sciences **107**, 13626 (2010).

[28] Y. Sumino, K. H. Nagai, Y. Shitaka, D. Tanaka, K. Yoshikawa, H. Chaté, and K. Oiwa, Nature **483**, 448 (2012).

[29] D. Bi, X. Yang, M. C. Marchetti, and M. L. Manning, Physical Review X **6**, 021011 (2016).

[30] G. Liu, A. Patch, F. Bahar, D. Yllanes, R. D. Welch, M. C. Marchetti, S. Thutupalli, and J. W. Shaevitz, Physical review letters **122**, 248102 (2019).

[31] G. Vásárhelyi, C. Virágh, G. Somorjai, T. Nepusz, A. E. Eiben, and T. Vicsek, Science Robotics **3** (2018).

[32] A. P. Solon, H. Chaté, and J. Tailleur, Physical Review Letters **114**, 068101 (2015).

[33] F. Ginelli and H. Chaté, Physical Review Letters **105**, 168103 (2010).

[34] T. Niizato and Y.-P. Gunji, Ecological Modelling **222**, 3041 (2011).

[35] J. Gautrais, F. Ginelli, R. Fournier, S. Blanco, M. Soria, H. Chaté, and G. Theraulaz, PLoS Comput Bio **8** (2012).

[36] A. Peshkov, S. Ngo, E. Bertin, H. Chaté, and F. Ginelli, Physical Review Letters **109**, 098101 (2012).

[37] M. Camperi, A. Cavagna, I. Giardina, G. Parisi, and E. Silvestri, Interface Focus **2**, 10.1098/rsfs.2012.0026 (2012).

[38] Y.-L. Chou, R. Wolfe, and T. Ihle, Physical Review E **86**, 021120 (2012).

[39] F. Ginelli, F. Peruani, M.-H. Pillot, H. Chaté, G. Theraulaz, and R. Bon, Proceedings of the National Academy of Sciences **112**, 12729 (2015).

[40] D. L. Barton, S. Henkes, C. J. Weijer, and R. Sknepnek, PLoS computational biology **13**, e1005569 (2017).

[41] P. Rahmani, F. Peruani, and P. Romanczuk, PLOS Computational Biology **16**, e1007697 (2020).

[42] M. Moussaïd, D. Helbing, and G. Theraulaz, Proceedings of the National Academy of Sciences **108**, 6884 (2011).

[43] H. Honda, M. Tanemura, and A. Yoshida, Acta biotheoretica **48**, 121 (2000).

[44] G. Schaller and M. Meyer-Hermann, Physical Review E **71**, 051910 (2005).

[45] M. Bock, A. K. Tyagi, J.-U. Kreft, and W. Alt, Bulletin of mathematical biology **72**, 1696 (2010).

[46] P. Rahmani, F. Peruani, and P. Romanczuk, arXiv preprint arXiv:2010.05902 (2020).

[47] E. Bertin, M. Droz, and G. Grégoire, Journal of Physics A: Mathematical and Theoretical **42**, 445001 (2009).

[48] J.-B. Caussin, A. Solon, A. Peshkov, H. Chaté, T. Dauxois, J. Tailleur, V. Vitelli, and D. Bartolo, Physical Review Letters **112**, 148102 (2014).

[49] A. Peshkov, E. Bertin, F. Ginelli, and H. Chaté, The European Physical Journal Special Topics **223**, 1315 (2014).

[50] T. Ihle, Journal of Statistical Mechanics: Theory and Experiment **2016**, 083205 (2016).

[51] See Supplemental Material [url], which includes theoretical and numerical details, as well as Refs. XXX.

[52] A. Solon, J.-B. Caussin, D. Bartolo, H. Chaté, and J. Tailleur, Physical review. E, Statistical, nonlinear, and soft matter physics **92 6**, 062111 (2015).

[53] A. B. Barbaro and P. Degond, Discrete & Continuous Dynamical Systems-B **19**, 1249 (2014).

[54] J. Barré, R. Chétrite, M. Muratori, and F. Peruani, Journal of

[55] D. Martin, H. Chaté, C. Nardini, A. Solon, J. Tailleur, F. van Wijland, *In preparation*.

[56] S. Nazarenko, N.-R. Kevlahan, and B. Dubrulle, Physica D: Nonlinear Phenomena **139**, 158 (2000).

[57] J. Marston, E. Conover, and T. Schneider, Journal of the Atmospheric Sciences **65**, 1955 (2008).

[58] F. Bouchet, C. Nardini, and T. Tangarife, Journal of Statistical Physics **153**, 572 (2013).

[59] N. A. Bakas and P. J. Ioannou, Journal of fluid mechanics **740**, 312 (2014).

[60] When α already depends on ρ, this shows the phase-separation scenario to be robust to the introduction of noise, in agreement with existing numerical results [4].

[61] A. P. Solon and J. Tailleur, Physical Review E **92**, 042119 (2015).

[62] See [67] for related, though different, models.

[63] D. Geyer, A. Morin, and D. Bartolo, Nature materials **17**, 789 (2018).

[64] L. Chen, J. Toner, and C. F. Lee, New Journal of Physics **17**, 042002 (2015).

[65] A. Cairoli and C. F. Lee, arXiv preprint arXiv:1904.08326 (2019).

[66] J. Delgado, Artificial intelligence **141**, 171 (2002).

[67] M. Aldana, V. Dossetti, C. Huepe, V. Kenkre, and H. Larralde, Physical review letters **98**, 095702 (2007).

Statistical Physics **158**, 589 (2015).